

MODELING PHARMACODYNAMICS ON HIV LATENT INFECTION: CHOICE OF DRUGS IS KEY TO SUCCESSFUL CURE VIA EARLY THERAPY*

NAVEEN K. VAIDYA[†] AND LIBIN RONG[‡]

Abstract. Highly active antiretroviral therapy has successfully controlled HIV replication in many patients. The treatment effectiveness may depend on the pharmacodynamics of antiretroviral drugs. In this paper, we integrate several drug-related parameters into an HIV infection model to investigate the effects of drug pharmacodynamics on the HIV latent reservoir and viral load dynamics. We showed that pharmacodynamic characteristics of drugs and the dosing schedule can significantly affect the outcome of either early or late treatment. Variations in each of the four studied parameters (the slope of the dose-response curve, the ratio of the maximum dosage to the 50% inhibitory concentration, the drug's half-life, and the dosing interval) can generate either an infection-free steady state or persistent infection when the other parameters remain unchanged. The global stability of the infection-free steady state and the viral persistence are shown to be governed by a viral invasion threshold that depends on the drug pharmacodynamics. Our results highlight that success of treatment, particularly pre-exposure prophylaxis or early treatment, may be determined by the choice of antiretroviral drugs in the treatment regimen; prophylaxis or very early treatment using drugs with a good pharmacodynamic profile has the potential to prevent or postpone the establishment of viral infection. In patients with established latent reservoir, late treatment can suppress the viral load to an undetectable level but cannot eradicate the virus. In this scenario, pharmacodynamic parameters and the dosing schedule can moderately change the viral load dynamics. However, the latent reservoir is hardly affected by them because it can be maintained by homeostasis of latently infected cells or other mechanisms rather than ongoing residual viral replication. These results support that drug pharmacodynamics need to be considered in studying HIV dynamics and in developing antiretroviral therapy against HIV infection.

Key words. HIV latent reservoir, periodic system, pharmacodynamics, reproductive number, time-varying drug effectiveness, viral invasion threshold

AMS subject classifications. 34D20, 37N25, 92B05, 92C50

DOI. 10.1137/16M1092003

1. Introduction. Human immunodeficiency virus (HIV) continues to be one of the biggest burdens in human health with about 37 million people living with the virus around the world and approximately 1.1 million deaths due to AIDS-related illness [49]. While there has been remarkable advancement in the development of antiretroviral therapy (ART) and prevention strategies, currently there is no cure for HIV. Therefore, the study towards the search for eradication of HIV is becoming increasingly important.

HIV infection establishes viral reservoirs in the form of cells or tissues that restrict virus replication and preserve replication-competent HIV for long periods of time [4]. Of these reservoirs, the latent proviral reservoir within resting CD4+ memory T cells constitutes the most challenging obstacle to viral eradication; currently available ART

*Received by the editors September 1, 2016; accepted for publication (in revised form) April 7, 2017; published electronically October 20, 2017.

<http://www.siam.org/journals/siap/77-5/M109200.html>

Funding: The research of the first author was supported by NSF grant DMS-1616299 and the start-up fund from San Diego State University. The research of the second author was partially supported by NSF grant DMS-1758290.

[†]Department of Mathematics and Statistics, San Diego State University, San Diego, CA 92182 (nvaidya@sdsu.edu, nvaidya.anyol@gmail.com).

[‡]Department of Mathematics, University of Florida, Gainesville, FL 32611 (libinrong@ufl.edu).

drugs are unable to affect latently infected cells. Such latently infected T-cells allow viral persistence despite immune surveillance or ART. These latent cells provide a continuous source of viremia following their activation by antigens [12]. Thus, a proper strategy for controlling latently infected cells is urgently needed.

Latent T-cell infection is established during early HIV infection [11, 28]. A study [3] on HIV patients treated early in infection showed that latently infected cells are mainly generated during primary infection from initiation of infection up to the time of ART, and once ART is initiated, there are many fewer infections generating fewer latently infected cells. This encouraging result suggests that the initiation of ART very early during infection can limit or possibly eradicate the virus, as supported by some successes of pre-exposure and post-exposure prophylaxis on avoiding infection [6, 13, 14, 18, 21, 36]. However, an experiment with simian immunodeficiency virus infected monkeys [48] showed that even the monkeys that were treated on day 3 postinfection suffer from virus rebound after discontinuation of ART following 24 weeks of fully suppressive therapy. Moreover, the accurate timing for establishment of a latent reservoir in humans is more uncertain [1]. Benefits of early therapy in controlling latently infected cells are not fully understood.

There are five major classes of HIV antiretroviral drugs [37, 38]: nucleoside reverse transcriptase inhibitors (NRTI), nonnucleoside reverse transcriptase inhibitors (NNRTI), protease inhibitors (PI), fusion inhibitors (FI), and integrase inhibitors (II). The absolute efficacy of these drugs *in vivo* has not been determined for the majority of drug regimes, and the efficacy can be as low as 68% for some combination therapies [24]. Such suboptimal treatment may result in viral rebound [19, 22, 38, 47], thereby providing an opportunity to establish latently infected cells even during treatment early in infection. Antiviral activity of treatment is mainly attributable to the pharmacodynamic properties of the drugs such as ED_{50} (drug concentration causing 50% inhibition) and the slope of the dose-response curve (the measure of how inhibition increases as a function of increasing drug concentration) [37, 38]. Moreover, the drug concentration in plasma varies widely and changes over time depending upon the drug's half-life, amount of drug intake, and adherence. Hence, the pharmacodynamics of drugs must be taken into account while designing treatment protocols that aim to mitigate HIV latent infection.

Many mathematical models have provided great insights into the dynamics of latently infected cells [3, 20, 33, 35]. However, there are very limited studies on virus and latent reservoir dynamics modeling with ART pharmacodynamics. In this study, we develop a mathematical model that incorporates a detailed pharmacodynamics of drugs to study effects of ART, particularly early ART, on controlling latently infected cells. We consider a realistic periodic drug intake scenario to obtain a periodic model system, and fully analyze the model to establish the local as well as the global properties of the infection dynamics. The invasion threshold, derived based on our model, is used to study the role of pharmacodynamic properties in eradicating viral infection. In addition, we present the latent infection dynamics influenced by the pharmacodynamic properties of drugs. Our study highlights that the pharmacodynamic properties, and thus the choice of drug combination, could be a determinant factor for successful eradication of HIV using early treatment strategy.

2. Model.

2.1. PLHI Model. We derive a pharmacodynamic latent HIV infection (PLHI) model by incorporating time-varying efficacy of ART into a latent viral dynamics model [29, 33]. A schematic diagram of the model is shown in Figure 1. As in

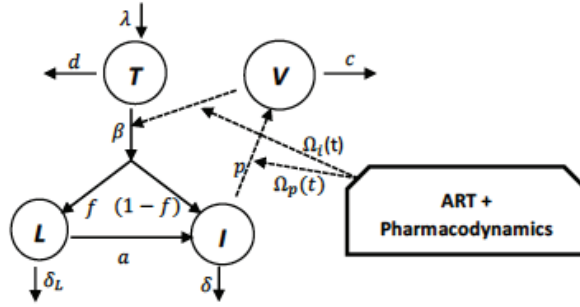


FIG. 1. Schematic diagram of PLHI model.

the previous models [29, 33], we consider three mutually exclusive compartments: uninfected target cells (T), productively infected cells (I), and latently infected cells (L). We further consider a compartment V that measures the concentration of free virus. We describe the infection dynamics using the following differential equations:

$$\begin{aligned}
 (1) \quad & \frac{dT}{dt} = \lambda - dT - \Omega_i(t)\beta VT, \quad T(0) = T_0, \\
 (2) \quad & \frac{dI}{dt} = (1-f)\Omega_i(t)\beta VT + aL - \delta I, \quad I(0) = I_0, \\
 (3) \quad & \frac{dL}{dt} = f\Omega_i(t)\beta VT - aL - \delta_L L, \quad L(0) = L_0, \\
 (4) \quad & \frac{dV}{dt} = \Omega_p(t)pI - cV, \quad V(0) = V_0.
 \end{aligned}$$

The target cells, T , die at rate d and are recruited into the infection cite at rate λ . Target cells become infected at a rate proportional to the product of target cell density and virus concentration with a rate constant β . We assume that a fraction, f , of infection generates latently infected cells with replication competent genomes and the remaining fraction of infection, $(1-f)$, leads to productively infected cells. Latently infected cells become productively infected at rate a due to activation. Productively infected cells produce new viruses at rate p per cell. Productively infected cells and latently infected cells die at rates δ and δ_L , respectively, while free viruses get cleared at rate c . The parameter values of the model used in this study are given in Table 1.

Currently available five classes of ART, FIs, NRTIs, NNRTIs, IIs, and PIs [37, 38], show their antiviral activity by reducing either the infection rate β to the rate $\Omega_i(t)\beta$ or the viral production rate p to the rate $\Omega_p(t)p$. Here, $\Omega_i(t)$ and $\Omega_p(t)$ are time-varying residual viral infectivity and viral production, respectively, during ART. Note that effectiveness of the drugs are given by $\epsilon_i(t) = 1 - \Omega_i(t)$ and $\epsilon_p(t) = 1 - \Omega_p(t)$.

2.2. Pharmacodynamic effects. Based on a classical dose-response relationship [7, 8, 37, 38], we formulate the residual viral infectivity, $\Omega_i(t)$, and the residual viral production, $\Omega_p(t)$, during ART as follows:

$$\begin{aligned}
 (5) \quad & \Omega_i(t) = \frac{1}{1 + [D_i(t)/ED_{50}^i]^{m_i}}, \\
 & \Omega_p(t) = \frac{1}{1 + [D_p(t)/ED_{50}^p]^{m_p}},
 \end{aligned}$$

TABLE 1
Model parameters.

Parameter	Description	Estimate	Source
λ	Recruitment rate of uninfected cells	10000 cells ml ⁻¹ day ⁻¹	[41]
d	Death rate of uninfected cells	0.01 day ⁻¹	[26, 41]
β	Infection rate	2×10^{-8} ml day ⁻¹	[32]
δ	Death rate of productively infected cells	1 day ⁻¹	[25]
f	Fraction of infection events generating latent infection	0.001	[35]
a	Activation rate of latently infected cells	0.2 day ⁻¹	[33]
δ_L	Death rate of latently infected cells	0.0039 day ⁻¹	[31, 50]
p	Virion production rate	4000 day ⁻¹	[33]
c	Virion clearance rate	23 day ⁻¹	[30]
ED_{50}^i, ED_{50}^p	Drug concentration for 50% efficacy	varied	
m_i, m_p	Hill's coefficients	varied	
k_i, k_p	Decay slope of the drug concentration	varied	
D_{max}^i, D_{max}^p	Maximum drug concentration	varied	
Δt	Drug intake interval	varied	

where m_i, m_p are Hill's coefficients, and ED_{50}^i and ED_{50}^p are the plasma concentrations of drugs required to obtain 50% of the maximal effect. Time-varying plasma concentrations of drugs, $D_i(t)$ and $D_p(t)$, are given by

$$(6) \quad \begin{aligned} D_i(t) &= D_{max}^i e^{-k_i(t-t_j)}, \\ D_p(t) &= D_{max}^p e^{-k_p(t-t_j)}, \\ t_j \leq t < t_{j+1}, \quad j &= 0, 1, 2, \dots, \end{aligned}$$

where $\Delta t = t_{j+1} - t_j$ represents drug intake interval, k_i, k_p are decay slopes of the drug concentrations, and D_{max}^i, D_{max}^p are maximum drug concentrations reached in the plasma following the drug intake. For simplicity, we assume the same D_{max}^i, D_{max}^p value after each drug intake, and consider the smooth spline functional curve accounting for impulses at dosing times followed by exponential decay (6). Therefore, the time-varying parameters $\Omega_i(t), \Omega_p(t)$ introduced into the model become smooth periodic functions of a period τ , i.e., $\Omega_i(t) = \Omega_i(t + \tau), \Omega_p(t) = \Omega_p(t + \tau)$, respectively. While the phase difference between drugs in a combination therapy can have impact as shown in previous modeling studies [5, 45], in today's practice most of the combined drugs are given at the same time [27]. Also, a single pill with multiple drugs has been developed and is widely used [27]. For this reason, we assume that all drugs combined are taken in the same interval of τ but this can be extended to a general case. In this periodic function, amplitude can be used to study the combined effect of maximum drug concentration reached in the plasma and the slope m , while the period can be used to study the average measure of drug intake intervals, including the average missed doses. For computational purposes, we consider the values of pharmacodynamics parameters from the experimentally estimated range that includes all five classes of HIV drugs [38]. While we vary parameters to study the effects of pharmacodynamics, we use Tenofovir, one of the drugs used in Truvada for pre-exposure prophylaxis, as our base case drug in the simulation. An example of time-varying drug concentration and time-varying residual viral activity during ART is shown in Figure 2.

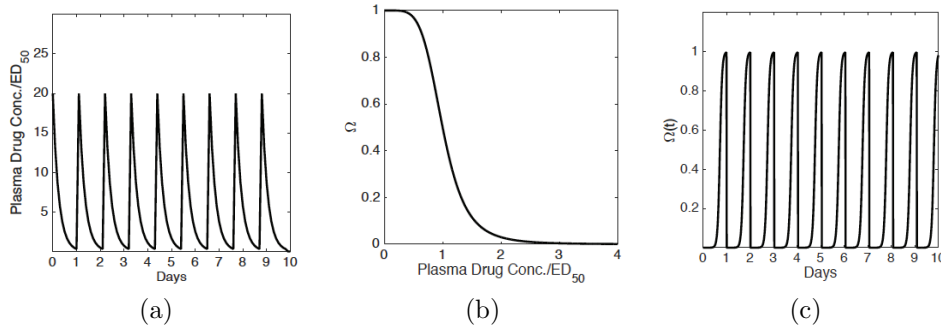


FIG. 2. (a) *Time-varying drug concentration*; (b) *residual viral activity during ART versus ART concentration*; and (c) *time-varying residual viral activity during ART*. The pharmacodynamic parameters used were $D_{max}/ED_{50} = 20$, half-life $t_{1/2} = 4$ hours, dosing interval $\tau = 1$ day, and $m = 2$.

3. Analytical results. For any $(T_0, I_0, L_0, V_0) \in \mathbb{R}_+^4$, system (1)–(4) has a unique local nonnegative solution $(T(t), I(t), L(t), V(t))$ through the initial value $(T(0), I(0), L(0), V(0)) = (T_0, I_0, L_0, V_0)$ [39]. Here, the dynamics of the total CD4+ T cells, $N(t) = T(t) + I(t) + L(t)$, is governed by $dN/dt = \lambda - dN - (\delta - d)I - (\delta_L - d)L \leq \lambda - \delta_L N$ as $\delta_L \ll d \ll \delta$. Note that the linear differential equation $dN/dt = \lambda - \delta_L N$ has a unique equilibrium $N^* = \lambda/\delta_L$, which is globally asymptotically stable. Then by the comparison principle [39], we obtain that $N(t)$ is ultimately bounded, and so are $T(t)$, $I(t)$, and $L(t)$. Also, since $\Omega_p(t) \leq 1$ and $I(t) \leq N(t)$, we get $dV/dt = \Omega_p(t)pI - cV \leq pN - cV$. Again, $dV/dt = pN - cV$ provides a limiting system $dV/dt = p\lambda/\delta_L - cV$, which has a globally asymptotically stable unique equilibrium $V^* = p\lambda/(\delta_L c)$. Then, by the comparison principle [40], $V(t)$ is also ultimately bounded. Hence, the solutions of the system (1)–(4) exist globally on the interval $[0, \infty)$. In summary, we have the following result.

THEOREM 3.1. *System (1)–(4) has a unique and bounded solution with the initial value $(T_0, I_0, L_0, V_0) \in \mathbb{R}_+^4$. Furthermore, for any $q > 0$, there exists $t_q > 0$ such that the solution of system (1)–(4) with $t \geq t_q$ lies in the compact set*

$$\mathbb{D}_{+q} = \{(T, I, L, V) \in \mathbb{R}_+^4 : N \leq \lambda/\delta_L + q, V \leq p\lambda/(\delta_L c) + q\}.$$

3.1. The basic reproductive number. The basic reproductive number, \mathcal{R}_0 , is defined as the average number of virus particles generated by a single virus particle introduced into a site with completely uninfected target cells. For a situation in which drug concentration can be maintained constant over time, \mathcal{R}_0 is a key threshold parameter that indicates—in the deterministic limit—if an infection is avoided or an infection occurs, depending upon whether its value exceeds one [2]. Using the next generation matrix approach [16, 44], we can derive the basic reproductive number for the PLHI model with constant residual viral activities $\bar{\Omega}_i, \bar{\Omega}_p$. The model system (1)–(4) has exactly one disease-free equilibrium $X_0 = (\lambda/d, 0, 0, 0)$, and equations for the infected cell and virus compartments of the linearized system at X_0 take the form

$$(7) \quad \frac{dI}{dt} = -\delta I + aL + \frac{\bar{\Omega}_i(1-f)\beta\lambda}{d}V,$$

$$(8) \quad \frac{dL}{dt} = -(a + \delta_L)L + \frac{\bar{\Omega}_i f \beta \lambda}{d}V,$$

$$(9) \quad \frac{dV}{dt} = \bar{\Omega}_p p I - cV.$$

We introduce the following matrices,

$$\mathcal{F} = \begin{pmatrix} 0 & 0 & \frac{\bar{\Omega}_i(1-f)\beta\lambda}{d} \\ 0 & 0 & \frac{\bar{\Omega}_i f \beta \lambda}{d} \\ 0 & 0 & 0 \end{pmatrix}, \quad \mathcal{V} = \begin{pmatrix} \delta & -a & 0 \\ 0 & a + \delta_L & 0 \\ -\bar{\Omega}_p p & 0 & c \end{pmatrix}.$$

These expressions give

$$\mathcal{F}\mathcal{V}^{-1} = \begin{pmatrix} \frac{\bar{\Omega}_i \bar{\Omega}_p (1-f) \beta \lambda p}{d \delta c} & \frac{\bar{\Omega}_i \bar{\Omega}_p (1-f) \beta \lambda p a}{d \delta c (a + \delta_L)} & 0 \\ \frac{\bar{\Omega}_i \bar{\Omega}_p f \beta \lambda p}{d \delta c} & \frac{\bar{\Omega}_i \bar{\Omega}_p f \beta \lambda p a}{d \delta c (a + \delta_L)} & 0 \\ 0 & 0 & 0 \end{pmatrix}.$$

Then \mathcal{R}_0 corresponds to the spectral radius of $\mathcal{F}\mathcal{V}^{-1}$:

$$\mathcal{R}_0 = \rho(\mathcal{F}\mathcal{V}^{-1}) = \frac{\bar{\Omega}_i \bar{\Omega}_p \beta \lambda p}{d \delta c} \left[1 - f + \frac{fa}{a + \delta_L} \right].$$

With the base-case parameters given in Table 1, in the absence of drugs, i.e., $\bar{\Omega}_i \bar{\Omega}_p = 1$, the basic reproductive number is $\mathcal{R}_0 = 3.5$. This shows that to avoid infection the combination drug efficacy $\bar{\epsilon} = 1 - \bar{\Omega}_i \bar{\Omega}_p$ should be maintained at a constant greater than $1 - 1/\mathcal{R}_0 = 0.71$, i.e., maintaining constant drug effectiveness of at least 71% should theoretically avoid infection. However, it is unlikely that the constant drug efficacy is maintained due to the time-varying nature of the plasma drug concentration and pharmacodynamic properties. Notice that in the presence of drugs, \mathcal{R}_0 is usually called the (on-treatment) reproductive number. For simplicity and comparison with other reproductive numbers discussed later, we still refer to it as the basic reproductive number.

3.2. The effective reproductive number. While \mathcal{R}_0 calculated above is useful to identify drug effectiveness that ensures that the virus does not grow at the beginning of the infection, the viral growth later during the infection may not be avoided because of the plasma drug concentration variations. To study the effect of plasma concentration over the time postinfection, a more relevant measure is the effective reproductive number, $\mathcal{R}_e(t)$. $\mathcal{R}_e(t)$ measures the average number of virus particles resulting from a single virus particle introduced at time t into the infection cite, given the uninfected target cell level at that time [9, 17]. For our model, $\mathcal{R}_e(t)$ is given by

$$R_e(t) = \Omega_i(t) \Omega_p(t) T(t) \frac{\beta p}{\delta c} \left[1 - f + \frac{fa}{a + \delta_L} \right].$$

To study the effects of pharmacodynamic parameters on the effective reproductive number, we plotted $R_e(t)$ with different parameters. For the ease of illustration, we used the combination drug efficacy $\epsilon(t) = 1 - \Omega_i(t) \Omega_p(t) = 1 - (1 - \epsilon_i(t)) \times (1 - \epsilon_p(t))$, which reduces the viral infection [34]. For the combination therapy, m is the corresponding slope of the dose-response curve, D_{max} is the maximum dosage, k is the decay rate of drug concentration, and τ is the dosing interval. Figure 3 shows the simulated $\mathcal{R}_e(t)$ with different slopes of the dose-response curve: (a) $m = 0.5$ and (b) $m = 3$. Figure 4 shows the simulated $\mathcal{R}_e(t)$ with different ratios of the maximum dosage to the 50% inhibitory concentration ED_{50} : (a) $n = D_{max}/ED_{50} = 10$ and (b) $n = 30$. In each figure, (c) and (d) are the same as (a) and (b), respectively,

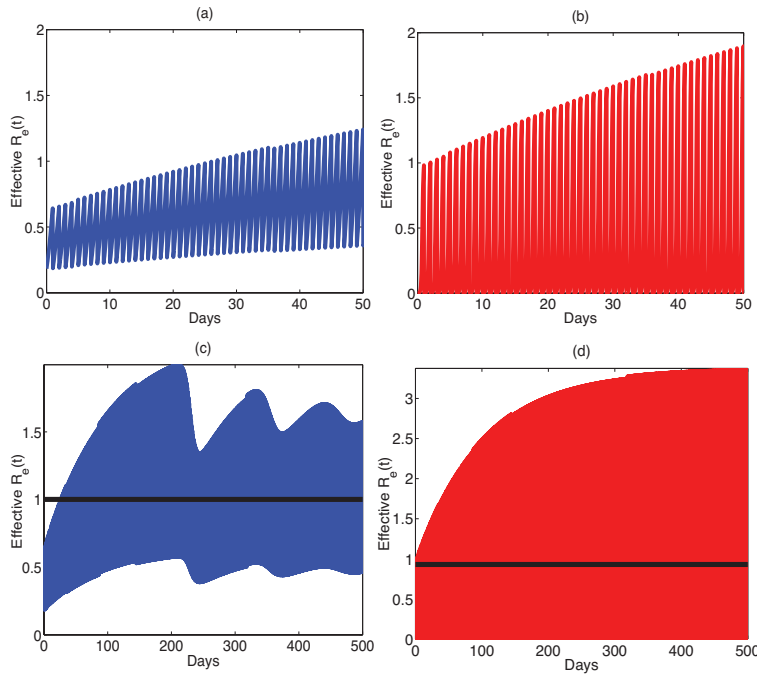


FIG. 3. The effective reproductive number $R_e(t)$ with different slopes of the dose-response curve: (a) $m = 0.5$ and (b) $m = 3$. (c) and (d) are the same as (a) and (b), respectively, but plotted over a longer period of time. The averages of the effective reproductive number are (c) $\bar{R}_e = 1.0011$ and (d) $\bar{R}_e = 0.9296$, which are plotted using black horizontal lines. The parameters $ED_{50} = 168.4$ nm, $n = 20$, half-life $t_{1/2} = 4$ hours, dosing interval $\tau = 1$ day were fixed. The other parameters were listed in Table 1.

but show the simulation over a longer time period so that the average of the effective reproductive number can be calculated (horizontal lines in (c) and (d)). Because of the decay of drug after each dose, the effective reproductive number undergoes extensive oscillations. In general, the amplitude of the oscillation increases as the slope of the dose-response curve increases or the ratio D_{max}/ED_{50} decreases. We will show the dynamics of the latent reservoir and viral load for each case later. The average of the effective reproductive number will be compared with the basic reproductive number calculated from the average of drug efficacy, and will also be evaluated to determine if it can predict the long-term dynamical behavior of the system.

3.3. Viral invasion threshold. Despite being a useful indicator for both the severity of an infection and the effort required to control the infection, one of the weaknesses of $\mathcal{R}_e(t)$ is that this number is not a threshold parameter for viral invasion [46]. We now derive a viral invasion threshold under ART, \mathcal{R}_i , using an approach similar to those in Wang and Zhao [46], Liu, Zhao, and Zhou [23], and Vaidya and Wahl [43].

For our τ -periodic PLHI model system, i.e., $\Omega_i(t) = \Omega_i(t + \tau)$, $\Omega_p(t) = \Omega_p(t + \tau)$, equations for the infected cells and virus compartments of the linearized system at the infection-free equilibrium, X_0 , take the form

$$(10) \quad \frac{dI}{dt} = -\delta I + aL + \frac{\Omega_i(t)(1-f)\beta\lambda}{d}V,$$

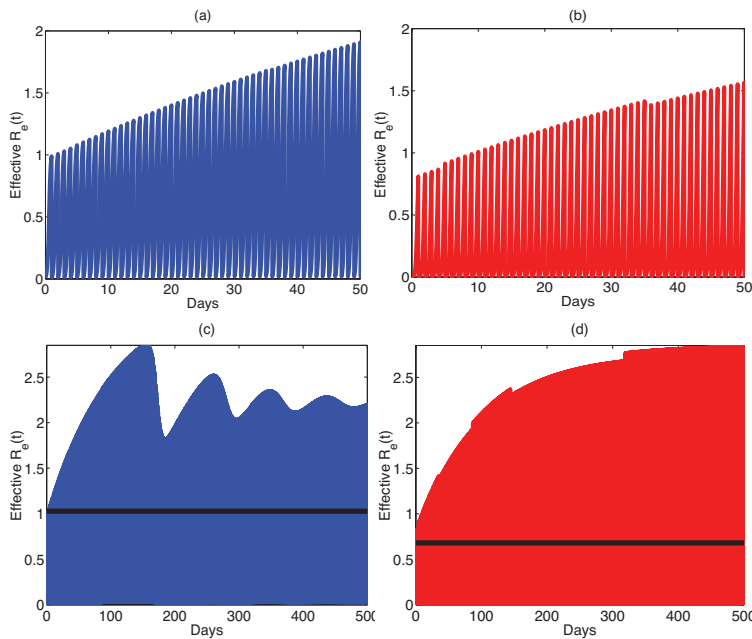


FIG. 4. The effective reproductive number $R_e(t)$ using different ratios of the maximum dosage to ED_{50} : (a) $n = D_{max}/ED_{50} = 10$ and (b) $n = 30$. (c) and (d) are the same as (a) and (b), respectively, but plotted over 500 days. The averages of the effective reproductive number are (c) $\bar{R}_e = 1.0272$ and (d) $\bar{R}_e = 0.6809$, which are plotted using black horizontal lines. The slope of the dose-response curve was fixed at $m = 2$ and the other parameters are the same as those in Figure 3.

$$(11) \quad \frac{dL}{dt} = -(a + \delta_L)L + \frac{\Omega_i(t)f\beta\lambda}{d}V,$$

$$(12) \quad \frac{dV}{dt} = \Omega_p(t)pI - cV.$$

We consider

$$\mathcal{F}_\tau = \begin{pmatrix} 0 & 0 & \frac{\Omega_i(t)(1-f)\beta\lambda}{d} \\ 0 & 0 & \frac{\Omega_i(t)f\beta\lambda}{d} \\ 0 & 0 & 0 \end{pmatrix}, \quad \mathcal{V}_\tau(t) = \begin{pmatrix} \delta & -a & 0 \\ 0 & a + \delta_L & 0 \\ -\Omega_p(t)p & 0 & c \end{pmatrix}.$$

We assume that $Y(t, s), t \geq s$, is the evolution operator of the linear τ -periodic system

$$(13) \quad \frac{dy}{dt} = -\mathcal{V}_\tau(t)y.$$

That is, for each $s \in \mathbb{R}$, the 3×3 matrix $Y(t, s)$ satisfies

$$\frac{d}{dt}Y(t, s) = -\mathcal{V}_\tau(t)Y(t, s) \quad \forall t \geq s, Y(s, s) = I,$$

where I is the 3×3 identity matrix. Then the monodromy matrix, $\Phi_{-\mathcal{V}_\tau}(t)$ of (13), is equal to $Y(t, 0), t \geq 0$.

Let $\varphi(s)$ be the initial distribution of virus particles. Then $\mathcal{F}_\tau\varphi(s)$ is the rate of new infected cells produced by the virus particles which were introduced at time

s . Given $t \geq s$, $Y(t, s)\mathcal{F}_\tau\varphi(s)$ provides the distribution of those virus particles which were newly produced by infected cells at time s and remain in the virus compartment at time t .

Let C_τ be the ordered Banach space of all τ -periodic functions from \mathbb{R} to \mathbb{R}^3 with the maximum norm $\|\cdot\|$ and the positive cone $C_\tau^+ := \{\varphi \in C_\tau : \varphi(t) \geq 0, \forall t \in \mathbb{R}\}$. We now define a linear operator $\mathcal{L} : C_\tau \rightarrow C_\tau$ by

$$(\mathcal{L}\varphi)(t) = \int_0^\infty Y(t, t-\xi)\mathcal{F}_\tau\varphi(t-\xi)d\xi \quad \forall t \in \mathbb{R}, \varphi \in C_\tau.$$

Here, $\int_0^\infty Y(t, t-\xi)\mathcal{F}_\tau\varphi(t-\xi)d\xi = \int_{-\infty}^t Y(t, s)\mathcal{F}_\tau\varphi(s)ds$ gives the distribution of accumulative new viruses at time t produced due to all those viruses $\varphi(s)$ at times before time t . Therefore, \mathcal{L} is the next infection operator [43, 46], and we define a viral invasion threshold as $\mathcal{R}_i = \rho(\mathcal{L})$, the spectral radius of \mathcal{L} .

As in Wang and Zhao [46] and Liu, Zhao and Zhou [23], we let $\mathcal{T}(t, \vartheta)$ be the monodromy matrix of the linear τ -periodic system

$$\frac{d\tau}{dt} = \left(-\mathcal{V}_\tau(t) + \frac{1}{\vartheta}\mathcal{F}_\tau \right) \tau, \quad t \in \mathbb{R},$$

with parameter $\vartheta \in (0, \infty)$. Since \mathcal{F}_τ is nonnegative and $-\mathcal{V}_\tau(t)$ is cooperative, it follows that $\lim_{\vartheta \rightarrow \infty} \rho(\mathcal{T}(\tau, \vartheta)) < 1$ and $\rho(\mathcal{T}(\tau, \vartheta))$ is continuous and nonincreasing in $\vartheta \in (0, \infty)$. Thus, as proved in Wang and Zhao [46], we have the following two results.

LEMMA 3.2. *The following statements hold [46].*

- (i) *If $\rho(\mathcal{T}(\tau, \vartheta)) = 1$ has a positive solution ϑ_0 , then ϑ_0 is an eigenvalue of operator \mathcal{L} , and hence $\mathcal{R}_i > 0$.*
- (ii) *If $\mathcal{R}_i > 0$, then $\vartheta = \mathcal{R}_i$ is the unique solution of $\rho(\mathcal{T}(\tau, \vartheta)) = 1$.*
- (iii) *$\mathcal{R}_i = 0$ if and only if $\rho(\mathcal{T}(\tau, \vartheta)) < 1$ for all $\vartheta > 0$.*

LEMMA 3.3 (see [46]). *The infection-free equilibrium X_0 is locally asymptotically stable if $\mathcal{R}_i < 1$, and unstable if $\mathcal{R}_i > 1$.*

3.4. Global dynamics: Viral persistence. By deriving a condition for the global stability of X_0 in the following theorem, we establish the condition for global eradication of the virus from the body.

THEOREM 3.4. *If $\mathcal{R}_i < 1$, then the unique infection-free equilibrium,*

$$X_0 = (\lambda/d, 0, 0, 0),$$

is globally asymptotically stable.

Proof. See Appendix A for the proof. □

We can also prove that $\mathcal{R}_i > 1$ provides a condition for the long-term HIV persistence in the body with at least one positive periodic solution. We state the result in the following theorem.

THEOREM 3.5. *If $\mathcal{R}_i > 1$, then there exists a value $\xi > 0$ such that any solution $(T(t), I(t), L(t), V(t))$ of the system (1)–(4) with the initial value $(T_0, I_0, L_0, V_0) \in \mathbb{D}_0 = \{(T, I, L, V) \in \mathbb{R}_+^4 : I > 0, L > 0, V > 0\}$ satisfies.*

$$\liminf_{t \rightarrow +\infty} I(t) \geq \xi, \quad \liminf_{t \rightarrow +\infty} L(t) \geq \xi, \quad \text{and} \quad \liminf_{t \rightarrow +\infty} V(t) \geq \xi,$$

and the system (1)–(4) admits at least one positive periodic solution.

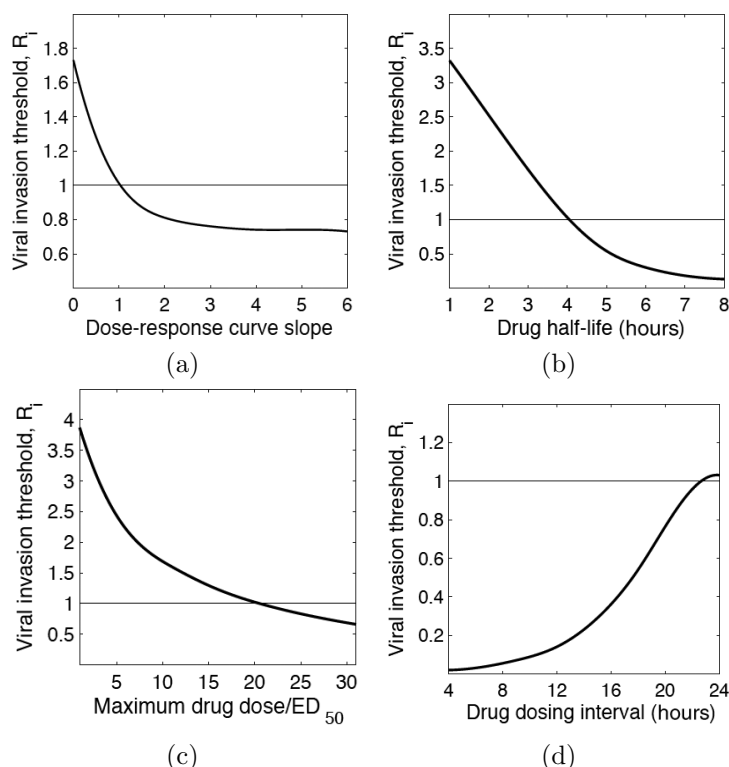


FIG. 5. The viral invasion threshold, \mathcal{R}_i , as a function of (a) the slope of dose-response curve, m , (b) the half-life of drugs, $t_{1/2}$, (c) the ratio of the maximum doses to the 50% inhibitory concentration, D_{max}/ED_{50} , and (d) the dosing interval, τ . In each case, remaining pharmacodynamic parameters were fixed at their base value, i.e., $D_{max}/ED_{50} = 20$, half-life $t_{1/2} = 4$ hours, dosing interval $\tau = 1$ day, and $m = 2$. The other viral dynamic parameters are listed in Table 1.

Proof. See Appendix B for the proof. \square

According to Lemma 3.2, \mathcal{R}_i can be obtained by solving $\rho(\mathcal{T}(\tau, \vartheta)) = 1$ for ϑ . Using this technique, we computed \mathcal{R}_i numerically to study how \mathcal{R}_i depends on the pharmacodynamic parameters m , k , D_{max}/ED_{50} , and τ (Figure 5). Each of these pharmacodynamic parameters can affect \mathcal{R}_i making it less than or greater than 1, thereby causing infection to die out or to persist. Drugs with a larger slope of the dose-response curve and a larger half-life are able to avoid the infection ($\mathcal{R}_i < 1$, Figures 5 (a), (b)). For example, in this particular simulation (Figures 5 (a), (b)), a slope of the dose-response curve greater than 1.2 and a half-life larger than 4 hours can bring \mathcal{R}_i below one. Moreover, to avoid infection (i.e., for $\mathcal{R}_i < 1$), the ratio of the maximum dose to ED_{50} needs to be high enough (for example, D_{max} needs to be at least 20 times higher than ED_{50} in our calculation; Figure 5 (c)), and the drug dosing interval cannot be too long (Figure 5 (d)). Therefore, missing doses can affect the success of treatment programs.

4. Effects of pharmacodynamics on HIV latent reservoir and virus dynamics: Model predictions.

4.1. Pre-exposure prophylaxis or early treatment. In this section, we used the PLHI model (1)–(4) to evaluate the influence of drug-related parameters and early treatment on the dynamics of latent reservoir and viral load. Treatment was assumed

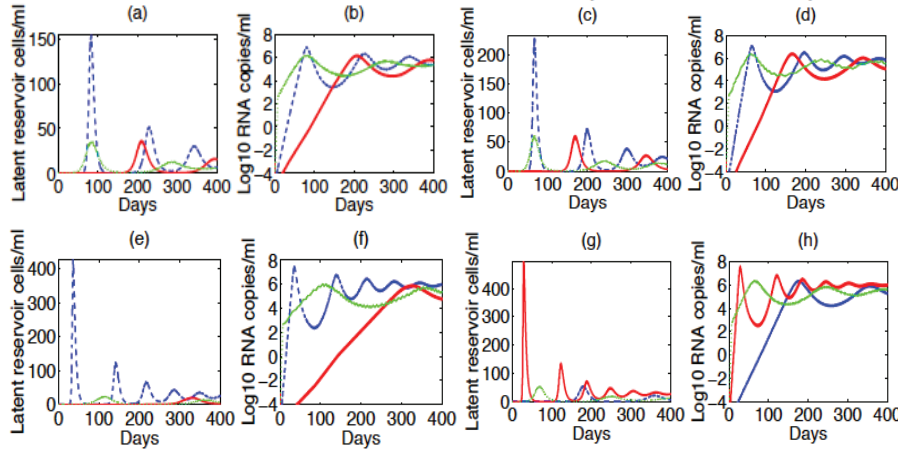


FIG. 6. Effects of early treatment and pharmacodynamic parameters on the latent reservoir (first and third column) and viral load (second and fourth column). ((a), (b)) Treatment is assumed to be given at the time of infection, i.e., $t = 0$ (blue dashed line for $m = 0.5$ and red solid line for $m = 1$) or given one week after infection, i.e., $t = 7$ days (green dotted line for $m = 1$); ((c), (d)) treatment is given at $t = 0$ (blue dashed line for $n = D_{max}/ED_{50} = 10$ and red solid line for $n = 15$) or $t = 7$ days (green dotted line for $n = 15$); ((e), (f)) treatment is given at $t = 0$ (blue dashed line for the half-life $t_{1/2} = 3$ hours and red solid line for $t_{1/2} = 5$ hours) or $t = 7$ days (green dotted line for $t_{1/2} = 5$ hours). The parameter $n = D_{max}/ED_{50}$ is fixed to be 10; ((g), (h)) treatment is given at $t = 0$ (blue dashed line for the dosing interval $\tau = 20$ hours and red solid line for $\tau = 40$ hours) or $t = 7$ days (green dotted line for $\tau = 20$ hours). The parameter n is also fixed to be 10 in (g), (h). All the other parameters are the same as those in Figure 3. Note that any combination of parameters that makes $\mathcal{R}_i < 1$ avoids viral infection and has no persistent curve on the latent reservoir and viral load graphs.

to be given at the time of infection or one week after infection. Different values of pharmacodynamic parameters and the dosing interval were used. We observe that for any combination of pharmacodynamic parameters that makes $\mathcal{R}_i < 1$, the infection is avoided and no persistent curve exists in the graphs of latent reservoir and viral load, consistent with the theoretical results above.

For pharmacodynamic parameters making $\mathcal{R}_i > 1$, the predicted dynamics of the latent reservoir and the viral load are shown in Figure 6. Using the slope of the dose-response curve as an example, a larger slope m led to a lower viral peak level and a longer time to the viral peak, as well as a smaller latent reservoir when treatment is given at the time of infection (blue dashed versus red solid line in Figures 6(a), (b)). With the same slope m , earlier treatment significantly postponed the establishment of the latent reservoir and viral infection (red solid versus green dotted line in Figures 6(a), (b)). Similarly, earlier therapy using drugs with a larger ratio n (Figures 6(c), (d)), a longer half-life $t_{1/2}$ (Figures 6(e), (f)) or a shorter dosing interval (Figures 6(g), (h)) was predicted to lower the magnitudes of the viral load and the latent reservoir size, and prolong the time needed to reach the viral peak during primary infection. In addition, all the simulations showed that earlier treatment with a better pharmacodynamic profile is always associated with more substantial suppression of the viral load and latently infected cells in the early stage of infection.

4.2. Late treatment during chronic infection. In this section, we explored the effects of pharmacodynamics of antiretroviral drugs on HIV latent reservoir and the viral load dynamics when the drug is initiated during chronic infection. Here also,

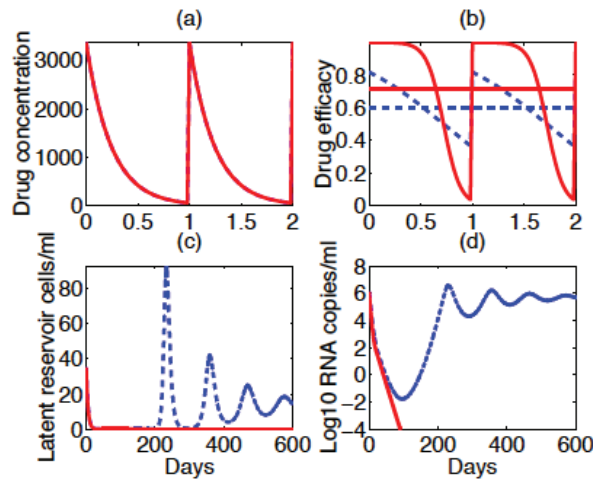


FIG. 7. The changes of drug concentration, drug efficacy, latent reservoir, and plasma viral load with different slopes of the dose-response curve $m = 0.5$ (blue dashed line) or $m = 3$ (red solid line). The averages of the drug efficacy, shown with horizontal lines in (b), are 0.6013 for $m = 0.5$ and 0.7127 for $m = 3$. The other parameter values are the same as those in Figure 3.

we investigated the influence of four drug-related parameters. The steady states of the model before treatment were used as the initial conditions of the model under treatment during chronic infection. In Figure 7, we plotted the predicted dynamics of drug concentration, drug efficacy, latent reservoir, and viral load with different slopes of the dose-response curve $m = 0.5$ (blue dashed line) or $m = 3$ (red solid line). We used the same drug concentration profile for both the slopes considered (Figure 7(a)). A larger slope m results in a higher initial drug efficacy and a slower initial decline although the drug efficacy declines to a lower level before the next dosage. The average of the drug efficacy is also higher for a larger slope m (Figure 7(b)). With $m = 0.5$, both the latent reservoir and the viral load persist (Figures 7(c), (d)). However, for a larger slope $m = 3$, both the latent reservoir and the viral load are predicted to die out. It is worth noticing that both the latent reservoir and the viral load experienced very frequent oscillations. The periodic forcing contributes to these frequent oscillations. It is not obviously seen in a figure over a long time period (Figures 7(c), (d)).

We are also interested in knowing if the basic reproductive number calculated by the average of drug efficacy ($R_0(\bar{e})$, denoted by \bar{R}_0) or even if the average effective reproductive number (\bar{R}_e) can provide a reasonable approximation to the viral invasion threshold, \mathcal{R}_i , and can determine the long-term viral dynamic behavior. When $m = 0.5$, the computed value of \mathcal{R}_i is 1.279 while the basic reproductive number using the average drug efficacy is 1.387 and the average of the effective reproductive number is $\bar{R}_e = 1.001$. The infection persists in this case. When m increases to 3, we estimate $\bar{R}_0 = 0.999$, $\bar{R}_e = 0.930$, and $\mathcal{R}_i = 0.761$, and the infection is predicted to die out. This suggests that for some drugs the values of \bar{R}_0 or \bar{R}_e may help to determine if the infection persists or dies out. This is consistent with the observation in an earlier study of HIV drug resistance using a two-strain model and time-varying drug efficacy [32]. However, the difference in the magnitudes of \bar{R}_0 or \bar{R}_e from \mathcal{R}_i shows that for some pharmacodynamic parameters, $\bar{R}_0 = 1$ or $\bar{R}_e = 1$ may not provide a reliable threshold value for the stability of the infection-free steady state.

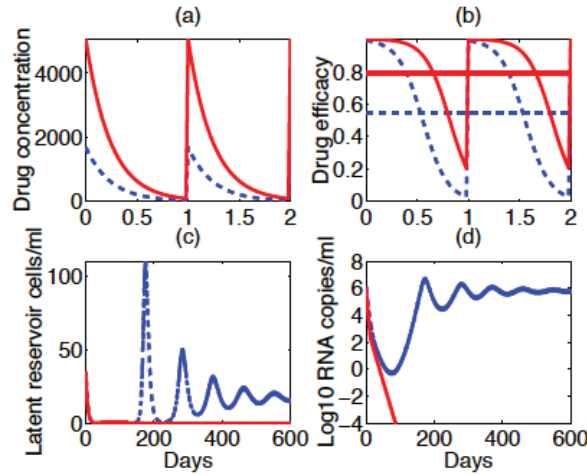


FIG. 8. Predicted dynamics of the model using different ratios of the maximum dosage to ED_{50} , i.e., $n = D_{max}/ED_{50} = 10$ (blue dashed line) or $n = 30$ (red solid line). The averages of the drug efficacy are 0.5467 for $n = 10$ and 0.7896 for $n = 30$. The slope of the dose-response curve was fixed to $m = 2$ and the other parameters are the same as those in Figure 3.

In Figure 8, we plotted the dynamics using different ratios of the maximum dosage to ED_{50} , i.e., $n = D_{max}/IC_{50} = 10$ (blue dashed line) or $n = 30$ (red solid line). A larger ratio n leads to a higher drug efficacy and lower levels of the latent reservoir and viral load. We also calculated the basic reproductive number using the average drug efficacy and found that $\bar{R}_0 = 1.5766$ for $n = 10$ and $\bar{R}_0 = 0.7318$ for $n = 30$. The average of the effective reproductive number is $\bar{R}_e = 1.0272$ for $n = 10$ and $\bar{R}_e = 0.6809$ for $n = 30$ (Figure 4). In this case, the value of infection invasion threshold is $\mathcal{R}_i = 1.688$ for $n = 10$ and $\mathcal{R}_i = 0.687$ for $n = 30$ (Figure 5).

We also showed the simulation with other drug-related parameters. For example, in Figure 9, the changes of drug concentration, efficacy, latent reservoir, and viral load were shown with different half-lives of antiretroviral drugs. The half-life of drug, $t_{1/2}$, was chosen to be 3 hours (blue dashed line) or 9 hours (red solid line). In Figure 10, we plotted the changes using different dosing intervals of antiretroviral drugs. The dosing interval τ is 12 hours (blue dashed line) or 36 hours (red solid line). With $t_{1/2} = 3$ hours, the average basic reproductive number is $\bar{R}_0 = 1.6189$ and the infection invasion threshold is $\mathcal{R}_i = 1.731$. The infection is predicted to be established. When $t_{1/2} = 9$ hours, the drug efficacy remains at a high level. The average basic reproductive number and the infection invasion threshold become $\bar{R}_0 = 0.0897$ and $\mathcal{R}_i = 0.130$, respectively, and the infection is predicted to die out (Figure 9). We had similar results when using different dosing intervals (Figure 10). For a longer dosing interval, for example, $\tau = 36$ hours (red solid line), the infection persists while for a shorter dosing interval, for example, $\tau = 12$ hours (blue dashed line in Figure 10), both the latent reservoir and virus are predicted to be eliminated.

From the simulations shown in Figures 7 to 10, we found that the pharmacodynamic parameters of drugs and the dosing schedule can play an important role in governing the dynamics of the latent reservoir and viral load. Variations in each of the four parameters (slope of the dose-response curve, ratio of the maximum dosage to ED_{50} , drug's half-life, and dosing interval) can generate either an infection-free steady state or persistent infection when all the other parameters remain unchanged.

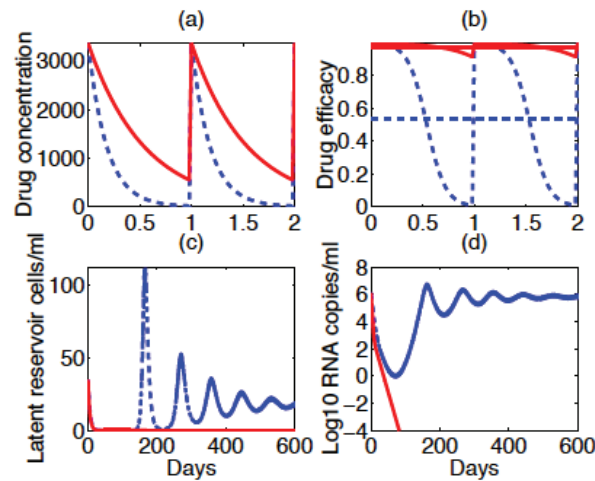


FIG. 9. Predicted changes of the drug concentration, efficacy, latent reservoir, and viral load using different half-lives of antiretroviral drugs. The half-life $t_{1/2}$ is 3 hours (blue dashed line) or 9 hours (red solid line). The averages of the drug efficacy are 0.5346 for $t_{1/2} = 3$ hours and 0.9742 for $t_{1/2} = 9$ hours. The slope of the dose-response curve was fixed at $m = 2$ and the other parameters are the same as those in Figure 3.

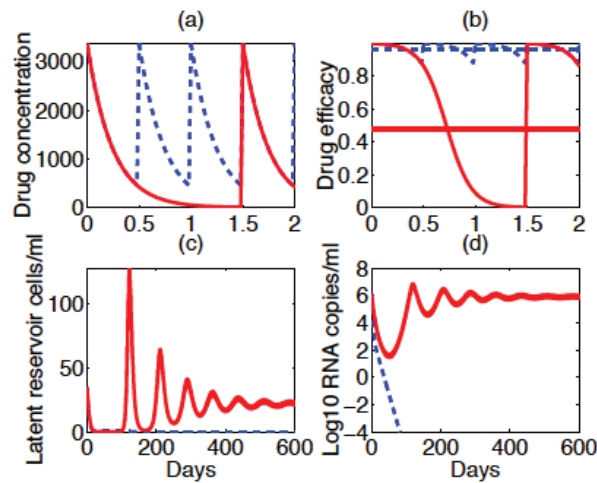


FIG. 10. Predicted dynamics using different dosing intervals of antiretroviral drugs. The dosing interval τ is 12 hours (blue dashed line) or 36 hours (red solid line). The averages of the drug efficacy are 0.9634 for $\tau = 12$ hours and 0.4769 for $\tau = 36$ hours. The slope of the dose-response curve was fixed to $m = 2$ and the other parameters are the same as those in Figure 3.

Simulations in Figures 7 to 10 show that a large slope of the dose-response curve, a large ratio of the maximum dosage to ED_{50} , a long half-life of drugs, or a frequent dosing schedule possibly clear the HIV latent infection. However, in reality, both the latent reservoir and the virus haven't been eliminated in patients despite a prolonged time of continuous combination ART during chronic infection. Proliferation of latently infected cells or the existence of drug sanctuaries where antiretroviral drugs have a poor penetrating ability and thus have minor antiviral activity may be the reason

for the latent reservoir and viral persistence. Homeostatic proliferation of latently infected cells was introduced in a mathematical model by Rong and Perelson in [35] and confirmed by an experimental study by Chomont et al. [10] to explain the stability of the latent reservoir and low viral load in patients on combination therapy. Here, using the same model we investigate the influence of drug-related parameters on the latent reservoir and virus after the viral load is suppressed to below the detection limit (i.e., 50 RNA copies/ml).

We used the same logistic term as in [35] to describe homeostatic proliferation of latently infected cells. The $L(t)$ equation (3) in the original model becomes the following,

$$(14) \quad \frac{dL}{dt} = f\Omega_i(t)\beta VT + \rho_m L \left(1 - \frac{L}{L_{max}}\right) - aL - \delta_L L.$$

The other equations for T , I , and V are unchanged. In the new equation for $L(t)$, ρ_m is the maximum proliferation rate and L_{max} is the carrying capacity concentration of latently infected cells. When the concentration of latently infected cells exceeds L_{max} , homeostatic proliferation shuts off. The model with this equation of latently infected cells was shown to be robust in generating a stable level of the latent reservoir, as well as a multiphasic viral load decline in patients receiving combination therapy [35].

Two additional parameters in (14), ρ_m and L_{max} , need to be determined for numerical simulation. For simplicity, the maximum proliferation rate ρ_m was chosen to be the sum of the activation rate, a , and the death rate, δ_L , of latently infected cells for the maintenance of the latent reservoir stability. The carrying capacity concentration of latently infected cells was set to 100 cells/ml according to the calculation in [35]. We also chose the viral production rate to be $p = 2000$ per day per infected cell in the simulation of this model in order for the viral load to be suppressed to below the detection limit after several months of therapy using the other parameters listed in Table 1.

In Figure 11, we plotted the predicted dynamics of both the latent reservoir and viral load using different parameters: ((a), (b)) the slope of the dose-response curve is $m = 0.5$ or $m = 3$; ((c), (d)) the ratio of the maximum dosage to ED_{50} is $n = 10$ or $n = 30$; ((e), (f)) the half-life of antiretroviral drugs is $t_{1/2} = 3$ hours or 9 hours; ((g), (h)) the dosing interval of antiretroviral drugs is $\tau = 12$ hours or 24 hours. With different pharmacodynamic parameters or dosing intervals, we found that the viral load is further lowered for a larger slope m , a larger ratio n , a longer half-life $t_{1/2}$, or a shorter dosing interval τ (Figure 11, second and forth columns). However, there is almost no influence of these parameters on the latent reservoir dynamics (Figure 11, first and third columns). This is not surprising because with the model including homeostasis of latency we assumed that the latent reservoir is mainly maintained by the homeostatic proliferation of latently infected cells rather than other mechanisms such as ongoing residual viral replication. Thus, once the treatment effectiveness is above a threshold value guaranteeing successful viral suppression, drug therapy has a minor effect on the decay of the latent reservoir. In the simulations, ongoing viral replication still partially contributes to the persistent viremia. Therefore, a more effective drug (e.g., with a larger slope m , a larger ratio n , a longer half-life $t_{1/2}$, or a more frequent dosing schedule) is able to suppress the viral load to a slightly lower level.

5. Discussion. Despite tremendous success of ART in controlling HIV replication, currently available anti-HIV drugs cannot cure the infection, mainly because of

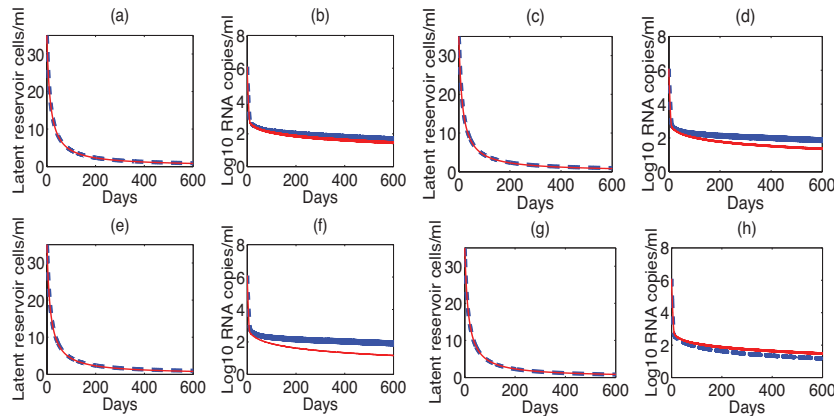


FIG. 11. Dynamics of the latent reservoir (first and third column) and viral load (second and fourth column) using the homeostasis model with different drug-related parameters. ((a), (b)) The slope of the dose-response curve is $m = 0.5$ (blue dashed line) or $m = 3$ (red solid line); ((c), (d)) The ratio of the maximum dosage to ED_{50} , i.e. $n = D_{max}/ED_{50} = 10$ (blue dashed line) or $n = 30$ (red solid line); ((e), (f)) The half life of antiretroviral drugs is 3 hours (blue dashed line) or 9 hours (red solid line); ((g), (h)) The dosing interval of antiretroviral drugs is 12 hours (blue dashed line) or 24 hours (red solid line). Except in Figure (a, b) in which the slope m of the dose-response curve varies, the slope was fixed to $m = 2$ in other figures. In addition, we fixed $\rho_m = a + \delta_L$, $L_{max} = 100$ cells/ml, $p = 2000$ per infected cell per day and all the other parameters are the same as those in Figure 3.

the establishment of viral reservoirs in the form of latently infected cells. Searching for the ways to reduce or eradicate the latent reservoir has been one of the major objectives of current HIV research. In this endeavor, early treatment (before infection or right after infection) to avoid the formation of such latently infected cells has recently gained significant attention. However, limited studies have documented contrasting results on benefits of early treatment in controlling latently infected cells; some studies with early treatment, including pre-exposure and post-exposure prophylaxis, have shown successful avoidance of infection while a recent study [48] on monkey experiments with treatment beginning at as early as 3 days postinfection showed viral rebound indicating the failure of early treatment to prevent the latent reservoir formation. The factors that determine the success of early treatment are poorly understood, and the pharmacodynamic properties of drugs, a potential explanation for treatment success, were ignored in previous studies.

The main objective of this study was to develop mathematical models to investigate effects of pharmacodynamics on the treatment outcomes. Thorough analysis and simulation of our models, including the periodic system with periodic drug intake, provided several interesting findings that can be beneficial to develop proper guidelines for successful treatment regimens. One of the major contributions of this study is a formulation of the infection invasion threshold, \mathcal{R}_i , that provides a condition for the global stability of the infection-free equilibrium in the situation of time-varying drug profile, i.e., the infection is predicted to die out if $\mathcal{R}_i < 1$ (Theorem 3.4) and the infection persists if $\mathcal{R}_i > 1$ (Theorem 3.5). Most importantly, we determined that the infection invasion threshold highly depends upon a few pharmacodynamic parameters (Figure 5) showing that the success of early treatment can be determined by the choice of drugs used in the treatment regimens. In particular, we found that the drugs with a larger slope of the dose-response curve, a larger ratio of the maximum drug dose to

50% inhibitory effect, and/or a higher half-life, can reduce \mathcal{R}_i , thereby increasing the probability of treatment success. Moreover, an increase in the drug-dosing interval increases \mathcal{R}_i . Therefore, only drugs with proper pharmacodynamic properties given in proper intervals can successfully avoid the infection. It's worth noting that the drugs used in the monkey experiments [48] with early treatment failure were NRTI and II, which have a small slope of the dose-response curve [38], indicating that our findings about the effects of pharmacodynamics may explain the mechanism for the treatment failure in that experiment.

Note that the different pharmacodynamic properties can provide quite different plasma drug concentration profiles (Figures 7–10), and the basic reproductive number, \mathcal{R}_0 , computed using the average of the periodic drug profile can be quite different from \mathcal{R}_i , highlighting the fact that \mathcal{R}_0 might not provide a reasonable threshold for infection persistence for some drugs. Not only do pharmacodynamic parameters of ART have an important role on achieving $\mathcal{R}_i < 1$ and preventing infection, but also these parameters significantly affect the viral and latent reservoir dynamics in the case of $\mathcal{R}_i > 1$ where the infection persists (Figure 6). For example, drugs with a larger slope of the drug-response curve result in a lower viral peak, a longer time to the viral peak, and a smaller latent reservoir size. Similar results were observed with the drugs having a larger ratio of maximum dose to ED_{50} , a longer half-life, and/or given in a shorter dosing interval. As in the case of pre-exposure prophylaxis, these effects of pharmacodynamic parameters on suppressing viral load and latently infected cells are also clearly seen in postinfection early treatment during primary infection. Therefore, these results suggest that prophylaxis or early treatment using antiretroviral drugs with good pharmacodynamic profiles has the potential to prevent or postpone the establishment of the latent reservoir and viral infection.

We also studied how pharmacodynamic properties affect the treatment outcomes when the treatment is initiated late during chronic infection (Figures 7–11). Importantly, during chronic infection when latently infected cells are already well established, the homeostatic proliferation of these cells becomes a substantial contributor to the viral dynamics [10, 35]. Therefore, for studying the late treatment outcomes, we extended our PLHI model to the one that includes homeostatic proliferation of latently infected cells. While in the absence of homeostatic proliferation the effect of pharmacodynamics of late treatment are similar to those of the early treatment (Figures 7–10), the homeostatic proliferation results in a quite different effect of pharmacodynamic properties on the latent reservoir (Figure 11). The latent reservoir dynamics remains almost unaffected by the drug pharmacodynamic properties. This is expected as the latent reservoir is primarily maintained by the process of homeostatic proliferation that is not affected by currently available drugs. However, because of a small amount of ongoing viral replication during late treatment, the viral load is further lowered by drugs with a better pharmacodynamic profile (Figure 11).

We acknowledge a few limitations of this study. Our results are based on the deterministic model. As the levels of latent infection and viral load are very low during treatment, stochastic factors may contribute to the elimination of latently infected cells and the virus in some patients even though the deterministic model always predicts the establishment of viral infection. Also, because of the deterministic nature, the model cannot distinguish asymptotic behavior between pre-exposure prophylaxis and early treatment as long as they both have the same drug pharmacodynamics properties even though the distinction is significant in their transient dynamics (Figures 6(a), (b)). Possible stochastic effects may be studied using stochastic differential equations [15], but such models may produce additional complications for analysis.

Since the information about the intracellular drug concentration is not available, we assumed that the intracellular drug concentration is proportional to the plasma drug concentration. Our quantitative predictions can be improved when the accurate temporal measure of the intracellular drug concentration becomes available. In some patients treatment fails because of the emergence of drug resistance. Our models need to be modified to study effects of pharmacodynamics on the dynamics of sensitive and resistant viral species in those patients. While our theoretical results generate some interesting ideas for developing treatment protocols, many of these results need to be supported by in vitro and in vivo experiments before actual recommendations can be offered in practice.

In conclusion, pharmacodynamics of drugs used in treatment regimens can be a key factor in avoiding infection as well as controlling viral load and latent reservoir. For a successful treatment, particularly pre-exposure prophylaxis and early treatment programs, pharmacodynamic properties must be considered carefully while making the choice of drugs to include in the treatment program.

Appendix A. Proof of Theorem 3.4. Let $\mathcal{R}_i < 1$. Then Lemma 3.3 implies that X_0 is locally asymptotically stable, i.e., $\rho(\Phi_{\mathcal{F}_\tau - \mathcal{V}_\tau}(\tau)) < 1$. We can choose $q_0 > 0$ small enough giving $\rho(\Phi_{\mathcal{F}_\tau - \mathcal{V}_\tau + \mathcal{M}_{q_0}}(\tau)) < 1$, where

$$\mathcal{M}_{q_0} = \begin{pmatrix} 0 & 0 & \Omega_i(t)(1-f)\beta q_0 \\ 0 & 0 & \Omega_i(t)f\beta q_0 \\ 0 & 0 & 0 \end{pmatrix}.$$

From (1), $dT/dt \leq \lambda - dT$. This implies that $T(t) \leq \hat{T}(t) \rightarrow \lambda/d$ as $t \rightarrow \infty$. Therefore, for $q_0 > 0$, there exists $t_{q_0} > 0$ such that $T(t) \leq \lambda/d + q_0 \forall t \geq t_{q_0}$. Then from system (2)–(4), we have

$$(15) \quad \frac{dI}{dt} \leq \Omega_i(t)(1-f)\beta V \left(\frac{\lambda}{d} + q_0 \right) - \delta I + aL,$$

$$(16) \quad \frac{dL}{dt} \leq \Omega_i(t)f\beta V \left(\frac{\lambda}{d} + q_0 \right) - (a + \delta_L)L,$$

$$(17) \quad \frac{dV}{dt} = \Omega_p(t)pI - cV.$$

Now, consider the following comparison system

$$(18) \quad \begin{pmatrix} d\hat{I}/dt \\ d\hat{L}/dt \\ d\hat{V}/dt \end{pmatrix} = (\mathcal{F}_\tau - \mathcal{V}_\tau + \mathcal{M}_{q_0}) \begin{pmatrix} \hat{I} \\ \hat{L} \\ \hat{V} \end{pmatrix}.$$

Then according to Zhang and Zhao [51], there exists a positive, τ -periodic function $(\bar{I}(t), \bar{L}(t), \bar{V}(t))^T$ such that $(\hat{I}(t), \hat{L}(t), \hat{V}(t))^T = e^{\Theta t}(\bar{I}(t), \bar{L}(t), \bar{V}(t))^T$ is a solution of system (18), where $\Theta = \ln \rho(\Phi_{\mathcal{F}_\tau - \mathcal{V}_\tau + \mathcal{M}_{q_0}}(\tau))/\tau$. Here, $\rho(\Phi_{\mathcal{F}_\tau - \mathcal{V}_\tau + \mathcal{M}_{q_0}}(\tau)) < 1 \Rightarrow \Theta < 0$, which implies $(\hat{I}(t), \hat{L}(t), \hat{V}(t))^T \rightarrow (0, 0, 0)^T$ as $t \rightarrow +\infty$. Therefore, the $(0, 0, 0)^T$ solution of system (18) is globally asymptotically stable.

For any nonnegative initial value $(I(0), L(0), V(0))^T$ of system (15)–(17), we can choose a sufficiently large $m > 0$ satisfying $(I(0), L(0), V(0))^T \leq m(\bar{I}(0), \bar{L}(0), \bar{V}(0))^T$. Clearly, $m(\hat{I}(t), \hat{L}(t), \hat{V}(t))^T = me^{\Theta t}(\bar{I}(t), \bar{L}(t), \bar{V}(t))^T$ is also a solution of (18). Then applying the comparison principle [40], we get $(I(t), L(t), V(t))^T \leq m(\hat{I}(t), \hat{L}(t), \hat{V}(t))^T$ for all $t > 0$. Therefore, we get $I(t) \rightarrow 0$, $L(t) \rightarrow 0$, and $V(t) \rightarrow 0$ as $t \rightarrow +\infty$. Then,

by the theory of asymptotic autonomous systems [42], we get $T(t) \rightarrow \lambda/d$ as $t \rightarrow +\infty$. Hence, $\mathcal{R}_i < 1$ gives a condition for X_0 to be globally asymptotically stable.

Appendix B. Proof of Theorem 3.5. Consider

$$\mathbb{D}_0 := \{(T, I, L, V) \in \mathbb{R}_+^4 : I > 0, L > 0, V > 0\} \quad \text{and} \quad \partial\mathbb{D}_0 := \mathbb{R}_+^4 \setminus \mathbb{D}_0.$$

Define the Poincaré map $P : \mathbb{R}_+^4 \rightarrow \mathbb{R}_+^4$ associated with system (1)–(4) by $P(z_0) = u(\tau, z_0) \quad \forall z_0 \in \mathbb{R}_+^4$, where $u(t, z_0)$ is the unique solution of system (1)–(4) with $u(0, z_0) = z_0 = (T_0, I_0, L_0, V_0)$. Then $P^n(z_0) = u(n\tau, z_0) \quad \forall n \geq 0$.

Let $\mathcal{R}_i > 1$. In this case, the infection-free equilibrium $X_0 = (\lambda/d, 0, 0, 0)$ is an isolated invariant set in \mathbb{R}_+^4 , and $W^s(X_0) \cap \mathbb{D}_0 = \emptyset$, where $W^s(X_0)$ is the stable set of X_0 , as stated in the following lemma.

LEMMA B.1. *If $\mathcal{R}_i > 1$, then there exists a $\sigma^* > 0$ such that for any $z_0 = (T_0, I_0, L_0, V_0) \in \mathbb{D}_0$ with $\|z_0 - X_0\| \leq \sigma^*$, we have*

$$\limsup_{n \rightarrow \infty} D(P^n(z_0), X_0) \geq \sigma^*,$$

where $D(Z, X)$ denotes the distance between Z and X in \mathbb{R}^4 .

Proof. Since $\mathcal{R}_i > 1$, Lemma 3.3 implies that X_0 is unstable, i.e., $\rho(\Phi_{\mathcal{F}_\tau - \nu_\tau}(\tau)) > 1$. We can choose $q_1 > 0$ small enough giving $\rho(\Phi_{\mathcal{F}_\tau - \nu_\tau - \mathcal{M}_{q_1}}(\tau)) > 1$, where

$$\mathcal{M}_{q_1} = \begin{pmatrix} 0 & 0 & \Omega_i(t)(1-f)\beta q_1 \\ 0 & 0 & \Omega_i(t)f\beta q_1 \\ 0 & 0 & 0 \end{pmatrix}.$$

Note that the equation $dT/dt = \lambda - dT$ has a unique equilibrium $T^* = \lambda/d$, which is globally attractive in \mathbb{R}_+ . Also, the following perturbed system,

$$(19) \quad \frac{d\hat{T}(t)}{dt} = \lambda - (d + \sigma\Omega_i(t)\beta)\hat{T}(t),$$

admits a unique solution

$$\hat{T}(t, \sigma) = e^{-dt} e^{-\sigma\beta \int_0^t \Omega_i(s) ds} \left[\hat{T}(0, \sigma) + \lambda \int_0^t e^{ds} e^{\sigma\beta \int_0^s \Omega_i(\eta) d\eta} ds \right]$$

through the arbitrary initial value $\hat{T}(0, \sigma)$, and has a unique periodic solution

$$\hat{T}^*(t, \sigma) = e^{-dt} e^{-\sigma\beta \int_0^t \Omega_i(s) ds} \left[\hat{T}^*(0, \sigma) + \lambda \int_0^t e^{ds} e^{\sigma\beta \int_0^s \Omega_i(\eta) d\eta} ds \right],$$

where

$$\hat{T}^*(0, \sigma) = \frac{\lambda \int_0^\tau e^{ds} e^{\sigma\beta \int_0^s \Omega_i(\eta) d\eta} ds}{e^{d\tau} e^{\sigma\beta \int_0^\tau \Omega_i(s) ds} - 1}.$$

Clearly, $|\hat{T}(t, \sigma) - \hat{T}^*(t, \sigma)| \rightarrow 0$ as $t \rightarrow \infty$. Thus, $\hat{T}^*(t, \sigma)$ is globally attractive on \mathbb{R}_+ . By the implicit function theorem, it follows that $\hat{T}^*(0, \sigma)$ is continuous in σ with $\lim_{\sigma \rightarrow 0} \hat{T}^*(0, \sigma) = T^* = \lambda/d$. The continuous dependence of the solution $\hat{T}^*(t, \sigma)$ on the initial condition and parameter value implies that there exists a sufficiently small σ_1 with $\hat{T}^*(t, \sigma) > T^* - q_1 \quad \forall \sigma \leq \sigma_1$ and all $t \in [0, \tau]$. By the periodicity of $\hat{T}^*(t, \sigma)$ and constant $T^* - q_1$, we see that $\hat{T}^*(t, \sigma) > T^* - q_1$ holds for all $\sigma \leq \sigma_1$ and all

$t \geq 0$. By the continuity of the solutions with respect to the initial values, there exists a $\sigma^* > 0$ such that any $z_0 \in \mathbb{D}_0$ with $\|z_0 - X_0\| \leq \sigma^*$ implies $\|u(t, z_0) - u(t, X_0)\| < \sigma_1 \forall t \in [0, \tau]$. We now prove that

$$\limsup_{n \rightarrow \infty} D(P^n(z_0), X_0) \geq \sigma^*.$$

If possible, suppose that

$$\limsup_{n \rightarrow \infty} D(P^n(z_0), X_0) < \sigma^*$$

for some $z_0 \in \mathbb{D}_0$. Without loss of generality we assume that

$$D(P^n(z_0), X_0) < \sigma^* \forall n \geq 0.$$

This implies, by continuity, that

$$\|u(t, P^n(z_0)) - u(t, X_0)\| < \sigma_1 \forall n \geq 0 \forall t \in [0, \tau].$$

Note that any $t \geq 0$ can be expressed as $t = n\tau + \tilde{t}$ with $\tilde{t} \in [0, \tau)$ and n , the largest integer less than or equal to t/τ . Therefore,

$$\|u(t, z_0) - u(t, X_0)\| = \|u(\tilde{t}, P^n(z_0)) - u(\tilde{t}, X_0)\| < \sigma_1 \forall t \geq 0.$$

Substituting $u(t, z_0) = (T(t), I(t), L(t), V(t))$ and $u(t, X_0) = X_0$, we obtain $I(t) < \sigma_1, L(t) < \sigma_1, V(t) < \sigma_1 \forall t \geq 0$. Then, from (1), we obtain

$$(20) \quad \frac{dT}{dt} \geq \lambda - (d + \Omega_i(t)\beta\sigma_1)T.$$

Take $\sigma = \sigma_1$. Since the periodic solution $\hat{T}^*(t, \sigma)$ of (19) is globally attractive on \mathbb{R}_+ and $\hat{T}^*(t, \sigma) > T^* - q_1$, we have $T(t) \geq T^* - q_1$ for sufficiently large t . Using this in (2)–(4), we obtain, for sufficiently large t , that

$$(21) \quad \frac{dI}{dt} \geq -\delta I + aL + \Omega_i(t)(1-f)\beta \left(\frac{\lambda}{d} - q_1 \right) V,$$

$$(22) \quad \frac{dL}{dt} \geq -(a + \delta_L)L + \Omega_i(t)f\beta \left(\frac{\lambda}{d} - q_1 \right) V,$$

$$(23) \quad \frac{dV}{dt} = \Omega_p(t)pI - cV.$$

Again, for a comparison system

$$(24) \quad \begin{pmatrix} d\hat{I}/dt \\ d\hat{L}/dt \\ d\hat{V}/dt \end{pmatrix} = (\mathcal{F}_\tau - \mathcal{V}_\tau - \mathcal{M}_{q_1}) \begin{pmatrix} \hat{I} \\ \hat{L} \\ \hat{V} \end{pmatrix},$$

there exists a positive τ -periodic function $(\bar{I}(t), \bar{L}(t), \bar{V}(t))^T$ so that $(\hat{I}(t), \hat{L}(t), \hat{V}(t))^T = e^{\Theta_1 t}(\bar{I}(t), \bar{L}(t), \bar{V}(t))^T$ is a solution of system (24), where $\Theta_1 = \ln \rho(\Phi_{\mathcal{F}_\tau - \mathcal{V}_\tau - \mathcal{M}_{q_1}}(\tau))/\tau$ [51]. Here, $\rho(\Phi_{\mathcal{F}_\tau - \mathcal{V}_\tau - \mathcal{M}_{q_1}}(\tau)) > 1 \Rightarrow \Theta_1 > 0$, which implies that, for nonnegative integer n , $(\hat{I}(n\tau), \hat{L}(n\tau), \hat{V}(n\tau))^T = e^{\Theta_1 n\tau}(\bar{I}(n\tau), \bar{L}(n\tau), \bar{V}(n\tau))^T \rightarrow (\infty, \infty, \infty)^T$ as $n \rightarrow \infty$.

For any nonnegative initial value $(I(0), L(0), V(0))^T$ of system (21)–(23), we can choose a small enough $m_1 > 0$ satisfying $(I(0), L(0), V(0))^T \geq m_1(\bar{I}(0), \bar{L}(0), \bar{V}(0))^T$. Clearly, $m_1(\hat{I}(t), \hat{L}(t), \hat{V}(t))^T = m_1 e^{\Theta_1 t}(\bar{I}(t), \bar{L}(t), \bar{V}(t))^T$ is also a solution of (24). Then applying the comparison principle [40], we get $(I(t), L(t), V(t))^T \geq m_1(\hat{I}(t), \hat{L}(t), \hat{V}(t))^T$ for all $t > 0$. Therefore, we get $I(n\tau) \rightarrow \infty, L(n\tau) \rightarrow \infty$, and $V(n\tau) \rightarrow \infty$ as $n \rightarrow \infty$, which is a contradiction. This completes the proof. \square

We know from Theorem 3.1 that $\{P^n\}_{n \geq 0}$ admits a global attractor in \mathbb{R}_+^4 . We now prove that $\{P^n\}_{n \geq 0}$ is uniformly persistent with respect to $(\mathbb{D}_0, \partial\mathbb{D}_0)$. For any $z_0 \in \mathbb{D}_0$, from (1) we have

$$(25) \quad T(t) = e^{-\int_0^t \varrho(\bar{s}) d\bar{s}} \left[T_0 + \lambda \int_0^t e^{\int_0^{\bar{s}_1} \varrho(\bar{s}) d\bar{s}} d\bar{s}_1 \right] \geq \lambda e^{-\int_0^t \varrho(\bar{s}) d\bar{s}} \int_0^t e^{\int_0^{\bar{s}_1} \varrho(\bar{s}) d\bar{s}} d\bar{s}_1 > 0 \quad \forall t > 0,$$

where $\varrho(t) = d + \Omega_i(t)\beta V(t)$. As generalized to nonautonomous systems [39], the irreducibility of the cooperative matrix

$$\tilde{M}(t) = \begin{pmatrix} -\delta & a & \Omega_i(t)(1-f)\beta T(t) \\ 0 & -(a + \delta_L) & \Omega_i(t)f\beta T(t) \\ \Omega_p(t)p & 0 & -c \end{pmatrix}$$

implies that $(I(t), L(t), V(t))^T \gg 0 \forall t > 0$. Thus both \mathbb{R}_+^4 and \mathbb{D}_0 are positively invariant. Clearly, $\partial\mathbb{D}_0$ is relatively closed in \mathbb{R}_+^4 .

Note that

$$(26) \quad M_\partial := \{z_0 \in \partial\mathbb{D}_0 : P^n(z_0) \in \partial\mathbb{D}_0, \forall n \geq 0\} = \{(T, 0, 0, 0) \in \mathbb{R}_+^4 : T \geq 0\},$$

i.e., for any $z_0 = (T_0, I_0, L_0, V_0) \in \{z_0 \in \partial\mathbb{D}_0 : P^n(z_0) \in \partial\mathbb{D}_0, \forall n \geq 0\}$, we have $I(n\tau) = L(n\tau) = V(n\tau) = 0 \forall n \geq 0$. If this is not true, then we can get some integer $n_1 \geq 0$ such that $(I(n_1\tau), L(n_1\tau), V(n_1\tau))^T > 0$. Then by taking $n_1\tau$ as an initial time, (25) gives $T(t) > 0 \forall t > n_1\tau$. As mentioned above, generalization to nonautonomous systems provides $(I(t), L(t), V(t))^T \gg 0 \forall t > n_1\tau$, where the initial value $(I(n_1\tau), L(n_1\tau), V(n_1\tau))^T > 0$. This gives $P^n(z_0) \in \mathbb{D}_0 \Rightarrow z_0 \notin \{z_0 \in \partial\mathbb{D}_0 : P^n(z_0) \in \partial\mathbb{D}_0, \forall n \geq 0\}$, which is a contradiction. Hence (26) is true.

Note that the infection-free equilibrium $X_0 = (\lambda/d, 0, 0, 0)$ is a unique fixed point of P in M_∂ . Moreover, from Lemma B.1, X_0 is an isolated invariant set in \mathbb{R}_+^4 and $W^s(X_0) \cap \mathbb{D}_0 = \emptyset$. Also, using $I = L = V = 0$ in system (1)–(4), the resulting linear nonhomogeneous equation $dT/dt = \lambda - dT$ admits a global asymptotic stable equilibrium λ/d . Note that every orbit in M_∂ approaches X_0 , and X_0 is acyclic in M_∂ . By Zhao [52], it follows that $\{P^n\}_{n \geq 0}$ is uniformly persistent with respect to $(\mathbb{D}_0, \partial\mathbb{D}_0)$, and the solutions of system (1)–(4) are uniformly persistent with respect to $(\mathbb{D}_0, \partial\mathbb{D}_0)$, i.e., there exists a $\xi > 0$ such that any solution $(T(t), I(t), L(t), V(t))$ of system (1)–(4) with initial value $(T_0, I_0, L_0, V_0) \in \mathbb{D}_0$ satisfies $\liminf_{t \rightarrow \infty} I(t) \geq \xi$, $\liminf_{t \rightarrow \infty} L(t) \geq \xi$, and $\liminf_{t \rightarrow \infty} V(t) \geq \xi$.

Furthermore, P has a fixed point $(T^*(0), I^*(0), L^*(0), V^*(0)) \in \mathbb{D}_0$ [52]. Then $T^*(0) \geq 0, I^*(0) > 0, L^*(0) > 0$, and $V^*(0) > 0$. Moreover, there exists some $\bar{t} \in [0, \tau]$ with $T^*(\bar{t}) > 0$. If this is not true, we have $T^*(\bar{t}) \equiv 0 \forall \bar{t} \in [0, \tau]$. Then, due to the periodicity of $T^*(t)$, we have $T^*(t) \equiv 0 \forall t \geq 0$. Then, from (1), $0 = \lambda > 0$, which is a contradiction. Thus we obtain

$$(27) \quad T^*(t) = e^{-\int_{\bar{t}}^t \varrho^*(\bar{s}) d\bar{s}} \left[T^*(\bar{t}) + \lambda \int_{\bar{t}}^t e^{\int_{\bar{t}}^{\bar{s}_1} \varrho^*(\bar{s}) d\bar{s}} d\bar{s}_1 \right] > 0 \forall t \in [\bar{t}, \bar{t} + \tau],$$

where $\varrho^*(t) = d + \Omega_i(t)\beta V^*(t)$. The periodicity of $T^*(t)$ implies that $T^*(t) > 0 \forall t \geq 0$. From (2)–(4), and the irreducibility of the cooperative matrix

$$\begin{pmatrix} -\delta & a & \Omega_i(t)(1-f)\beta T^*(t) \\ 0 & -(a + \delta_L) & \Omega_i(t)f\beta T^*(t) \\ \Omega_p(t)p & 0 & -c \end{pmatrix},$$

we get $(I^*(t), L^*(t), V^*(t)) \in \text{Int}(\mathbb{R}_+^3) \forall t \geq 0$. Therefore, $(T^*(t), I^*(t), L^*(t), V^*(t))$ is a positive τ -periodic solution of system (1)–(4).

REFERENCES

- [1] J. ANANWORANICHA, K. DUBÉ, AND N. CHOMONT, *How does the timing of antiretroviral therapy initiation in acute infection affect HIV reservoirs?*, *Curr. Opin. HIV AIDS*, 10 (2015), pp. 18–28.
- [2] R. M. ANDERSON AND R. M. MAY, *Infectious Diseases of Humans: Dynamics and Control*, Oxford University Press, Oxford, 1991.
- [3] N. M. ARCHIN, N. K. VAIDYA, J. D. KURUCA, A. L. LIBERTYA, A. WIEGANDD, M. F. KEARNEYD, M. S. COHENA, J. M. COFFINE, R. J. BOSCHF, C. L. GAYA, J. J. ERONA, D. M. MARGOLISA, AND A. S. PERELSON, *Immediate antiviral therapy appears to restrict resting CD4+ cell HIV-1 infection without accelerating the decay of latent infection*, *Proc. Natl. Acad. Sci. USA*, 109 (2012), pp. 9523–9528.
- [4] J. N. BLANKSON, D. PERSAUD, AND R. F. SILICIANO, *The challenge of viral reservoirs in HIV-1 infection*, *Annu. Rev. Med.*, 53 (2002), pp. 557–593.
- [5] C. J. BROWNE AND S. S. PILYUGIN, *Periodic multi-drug therapy in a within-host virus model*, *Bull. Math. Biol.*, 74 (2012), pp. 562–589.
- [6] D. M. CARDO ET AL., *A case-control study of HIV seroconversion in health care workers after percutaneous exposure*, *New Engl. J. Med.*, 337 (1997), pp. 1485–1490.
- [7] T. C. CHOU, *Derivation and properties of Michaelis-Menten type and Hill type equations for reference ligands*, *J. Theoret. Biol.*, 59 (1976), pp. 253–276.
- [8] T. C. CHOU AND P. TALALAY, *Quantitative analysis of dose-effect relationships: The combined effects of multiple drugs or enzyme inhibitors*, *Adv. Enzyme Regul.*, 22 (1984), pp. 27–55.
- [9] A. CINTRON-ARIAS, C. CASTILLO-CHAVEZ, L. M. A. BETTENCOURT, A. L. LLOYD, AND H. T. BANKS, *The estimation of the effective reproductive number from disease outbreak data*, *Math. Biosci. Eng.*, 6 (2009), pp. 261–282.
- [10] N. CHOMONT ET AL., *HIV reservoir size and persistence are driven by T cell survival and homeostatic proliferation*, *Nature. Med.*, 15 (2009), pp. 893–900.
- [11] T. W. CHUN, D. ENGEL, M. M. BERREY, T. SHEA, L. COREY, AND A. S. FAUCI, *Early establishment of a pool of latently infected, resting CD4 (+) T cells during primary HIV-1 infection*, *Proc. Natl. Acad. Sci. USA*, 95 (1998), pp. 8869–8873.
- [12] T. W. CHUN, D. ENGEL, S. B. MIZELL, L. A. EHLER, AND A. S. FAUCI, *Induction of HIV-1 replication in latently infected CD4+ T cells using a combination of cytokines*, *J. Exp. Med.*, 188 (1998), pp. 83–91.
- [13] J. COHEN, *HIV/AIDS clinical trials: A powerful and perplexing new HIV prevention tool*, *Science*, 330 (2010), pp. 1298–1299.
- [14] E. M. CONNOR ET AL., *Reduction of maternal-infant transmission of human immunodeficiency virus type 1 with zidovudine treatment*, *N. Engl. J. Med.*, 331 (1994), pp. 1173–1180.
- [15] J. M. CONWAY, B. P. KONRAD, AND D. COOMBS, *Stochastic analysis of pre- and postexposure prophylaxis against HIV infection*, *SIAM J. Appl. Math.* 73 (2013), pp. 904–928.
- [16] O. DIEKMANN, J. A. HEESTERBEEK, AND J. A. METZ, *On the definition and the computation of the basic reproduction ratio R_0 in models for infectious diseases in heterogeneous populations*, *J. Math. Biol.*, 28 (1990), pp. 365–381.
- [17] C. P. FARRINGTON AND H. J. WHITAKER, *Estimation of effective reproduction numbers for infectious diseases using serological survey data*, *Biostatistics*, 4 (2003), pp. 626–632.
- [18] L. A. GUAY ET AL., *Intrapartum and neonatal single-dose nevirapine compared with zidovudine for prevention of mother-to-child transmission of HIV-1 in Kampala Uganda HIVNET 012 randomised trial*, *Lancet*, 354 (1999), pp. 795–802.
- [19] D. D. HO, A. U. NEUMANN, A. S. PERELSON, W. CHEN, J. M. LEONARD, AND M. MARKOWITZ, *Rapid turnover of plasma virions and CD4 lymphocytes in HIV-1 infection*, *Nature*, 373 (1995), pp. 123–126.
- [20] H. KIM AND A. S. PERELSON, *Viral and latent reservoir persistence in HIV-1-infected patients on therapy*, *PLoS Comput. Biol.*, 2 (2006), e135.
- [21] A. D. M. KASHUBA, K. B. PATTERSON, J. B. DUMOND, AND M. S. COHEN, *Pre-exposure prophylaxis for HIV prevention: How to predict success*, *Lancet*, 379 (2012), pp. 2409–2411.
- [22] B. A. LARDER, G. DARBY, AND D. D. RICHMAN, *HIV with reduced sensitivity to zidovudine (AZT) isolated during prolonged therapy*, *Science*, 243 (1989), pp. 1731–1734.

- [23] L. LIU, X. Q. ZHAO, AND Y. ZHOU, *A tuberculosis model with seasonality*, Bull. Math. Biol., 72 (2010), pp. 931–952.
- [24] M. LOUIE ET AL., *Determining the relative efficacy of highly active antiretroviral therapy*, J. Infect. Dis., 187 (2003), pp. 896–900.
- [25] M. MARKOWITZ, M. LOUIE, A. HURLEY, E. SUN, AND M. DI MASCIO, *A novel antiviral intervention results in more accurate assessment of human immunodeficiency virus type 1 replication dynamics and T-cell decay in vivo*, J. Virol., 77 (2003), pp. 5037–5038.
- [26] H. MOHRI, S. BONHOEFFER, S. MONARD, A. S. PERELSON, AND D. D. HO, *Rapid turnover of T lymphocytes in SIV-infected rhesus macaques*, Science, 279 (1998), pp. 1223–1227.
- [27] POZ, *2016 HIV Drug Chart*, <https://www.poz.com/article/2016-hiv-drug-chart> (2016).
- [28] A. NOE, J. PLUM, AND C. VERHOFSTEDE, *The latent HIV-1 reservoir in patients undergoing HAART: An archive of pre-HAART drug resistance*, J. Antimicrob. Chemother., 55 (2005), pp. 410–412.
- [29] A. S. PERELSON, P. ESSUNGER, Y. CAO, M. VESANEN, A. HURLEY, K. SAKSELA, M. MARKOWITZ, AND D. D. HO, *Decay characteristics of HIV-1-infected compartments during combination therapy*, Nature, 387 (1997), pp. 188–191.
- [30] B. RAMRATNAM, S. BONHOEFFER, J. BINLEY, A. HURLEY, L. ZHANG, J. E. MITTLER, M. MARKOWITZ, J. P. MOORE, A. S. PERELSON, AND D. D. HO, *Rapid production and clearance of HIV-1 and hepatitis C virus assessed by large volume plasma apheresis*, Lancet, 354 (1999), pp. 1782–1785.
- [31] B. RAMRATNAM, J. E. MITTLER, L. ZHANG, D. BODEN, A. HURLEY, F. FANG, C. A. MACKEN, A. S. PERELSON, M. MARKOWITZ, AND D. D. HO, *The decay of the latent reservoir of replication-competent HIV-1 is inversely correlated with the extent of residual viral replication during prolonged anti-retroviral therapy*, Nature. Med., 6 (2000), pp. 82–85.
- [32] L. RONG, Z. FENG, AND A. S. PERELSON, *Emergence of HIV-1 drug resistance during antiretroviral treatment*, Bull. Math. Biol., 69 (2007), pp. 2027–2060.
- [33] L. RONG AND A. S. PERELSON, *Modeling HIV persistence, the latent reservoir, and viral blips*, J. Theoret. Biol., 260 (2009), pp. 308–331.
- [34] L. RONG AND A. S. PERELSON, *Asymmetric division of activated latently infected cells may explain the decay kinetics of the HIV-1 latent reservoir and intermittent viral blips*, Math. Biosci., 217 (2009), pp. 77–87.
- [35] L. RONG AND A. S. PERELSON, *Modeling latently infected cell activation: Viral and latent reservoir persistence, and viral blips in HIV-infected patients on potent therapy*, PLoS Comput. Biol., 5 (2009), e1000533.
- [36] N. SHAFFER ET AL., *Short-course zidovudine for perinatal HIV-1 transmission in Bangkok, Thailand: A randomized controlled trial*, Lancet, 353 (1999), pp. 773–780.
- [37] L. SHEN, S. ALIREZA RABI, A. R. SEDAGHAT, L. SHAN, J. LAI, S. XING, AND R. F. SILICIANO, *A critical subset model provides a conceptual basis for the high antiviral activity of major HIV drugs*, Sci. Transl. Med., 3 (2011), 91ra63.
- [38] L. SHEN, S. PETERSON, A. R. SEDAGHAT, M. A. MCMAHON, M. CALLENDER, H. ZHANG, Y. ZHOU, E. PITT, K. S. ANDERSON, E. P. ACOSTA, AND R. F. SILICIANO, *Dose-response curve slope sets class-specific limits on inhibitory potential of anti-HIV drugs*, Nature. Med., 14 (2008), pp. 762–766.
- [39] H. L. SMITH, *Monotone Dynamical Systems: An Introduction to the Theory of Competitive and Cooperative Systems*, Math. Surveys Monogr. 41, Amer. Math. Soc., Providence, RI, 1995.
- [40] H. L. SMITH AND P. WALMAN, *The Theory of the Chemostat*, Cambridge University Press, Cambridge, 1995.
- [41] M. A. STAFFORD, L. COREY, Y. CAO, E. S. DAAR, D. D. HO, AND A. S. PERELSON, *Modeling plasma virus concentration during primary HIV infection*, J. Theoret. Biol., 203 (2000), pp. 285–301.
- [42] H. R. THIEME, *Convergence results and a Poincaré-Bendixson trichotomy for asymptotically autonomous differential equations*, J. Math. Biol., 30 (1992), pp. 755–763.
- [43] N. K. VAIDYA AND L. M. WAHL, *Avian influenza dynamics under periodic environmental conditions*, SIAM J. Appl. Math., 75 (2015), pp. 443–467.
- [44] P. VAN DEN DRIESSCHE AND J. WATMOUGH, *Reproduction numbers and sub-threshold endemic equilibria for compartmental models of disease transmission*, Math. Biosci., 180 (2002), pp. 29–48.
- [45] Z. WANG AND X. Q. ZHAO, *A within-host virus model with periodic multi-drug therapy*, Bull. Math. Biol., 75 (2013), pp. 543–563.
- [46] W. WANG AND X. Q. ZHAO, *Threshold dynamics for compartmental epidemic models in periodic environments*, J. Dynam. Differential Equations, 20 (2008), pp. 699–717.

- [47] X. WEI ET AL., *Viral dynamics in human immunodeficiency virus type 1 infection*, *Nature*, 373 (1995), pp. 117–122.
- [48] J. B. WHITNEY ET AL., *Rapid seeding of the viral reservoir prior to SIV viraemia in rhesus monkeys*, *Nature*, 512 (2014), pp. 74–77.
- [49] WHO, *HIV/AIDS*, <http://www.who.int/hiv/data/en> (2015).
- [50] L. ZHANG ET AL., *Quantifying residual HIV-1 replication in patients receiving combination antiretroviral therapy*, *N. Engl. J. Med.*, 340 (1999), pp. 1605–1613.
- [51] F. ZHANG AND X.-Q. ZHAO, *A periodic epidemic model in a patchy environment*, *J. Math. Anal. Appl.*, 325 (2007), pp. 496–516.
- [52] X.-Q. ZHAO, *Dynamical Systems in Population Biology*, Springer, New York, 2003.